NPL National Physical Laboratory

Report

NPL REPORT ENG 1

The development of artefacts for the gravimetric measurement of the density of moist air

J Berry, S Davidson and S Brown

NOT RESTRICTED

MAY 2007

National Physical Laboratory | Hampton Road | Teddington | Middlesex | United Kingdom | TW11 0LW

Switchboard 020 8977 3222 | **NPL Helpline** 020 8943 6880 | **Fax** 020 8943 6458 | **www.npl.co.uk**

The development of artefacts for the gravimetric measurement of the density of moist air

J Berry, S Davidson and S Brown
Industry & Innovation Division

ABSTRACT

High accuracy air density measurements are needed in calibrations of OIML E1 and E2 class mass standards, becoming more vital when calibrating a secondary stainless steel mass standard from a primary platinum-iridium (Pt-Ir) standard due to the large difference in volume between them. Current state of the art air density measurements using the conventional CIPM-81/91 method can measure air density to about 1 part in 10^4 (k = 1). However, gravimetric air density artefacts offer the opportunity to measure moist air density to about 1 part in 10^5 (k = 1), which would reduce the uncertainty on stainless steel – Pt-Ir calibrations by up to 50%. The moist air density measurements made using gravimetric artefacts presented in this report have demonstrated excellent agreement with the CIPM-81/91 method and offer an improved uncertainty of 1.1 parts in 10^5 (k = 1).

ISSN 1754-2987

National Physical Laboratory
Hampton Road, Teddington, Middlesex, TW11 0LW

Approved on behalf of the Managing Director, NPL,
by Dr Mark Gee, Knowledge Leader, Engineering Measurement Team, authorised by
Mrs Susan Evans, Director, Industry & Innovation Division

CONTENTS

1. INTRODUCTION

This report summarizes an evaluation of a method for the determination of the density of moist air using physical artefacts. The conventional method, as recommended by the International Committee for Weights and Measures (CIPM), requires the measurement of the air's temperature, pressure, relative humidity and carbon dioxide concentration, which are used in the CIPM-81/91 equation (derived by Giacomo [1] and modified by Davis [2]) to calculate the air density. In this manner, the density of moist air may be determined with an uncertainty of about 1 part in 10^4 (k=1). This provides the main uncertainty contribution when calibrating secondary stainless steel standards against primary platinum/iridium (Pt-Ir) standards [3] and therefore in the dissemination of the unit of mass at 1 kg. A reduction in the uncertainty of measuring the density of air to 1 part in 10^5 would halve the uncertainty when calibrating 1 kg stainless steel mass standards, and would also have the benefit of reducing the uncertainty in the mass calibration of weights further down the calibration chain [3] and for artefacts that are made from materials other than stainless steel and Pt-Ir, such as silicon [4]. The work on gravimetric air density artefacts presented in this report has demonstrated agreement with the CIPM-81/91 equation (corrected for the new Argon content in standard air value [5]) to 1 part in 10^4 and has reduced the uncertainty to around 1.5 parts in 10^5 (1. Improves uncertainty in measuring air density 2. Agrees within combined uncertainties with old method).

2. BACKGROUND

2.1 The need for air density measurement

The primary use for accurate air density measurements at the NPL is when disseminating the UK’s mass scale. The comparison of kilogram weights made from Pt-Ir material (such as the UK's national standard, kilogram 18) with those made from stainless steel - from which the majority of laboratory and industrial standards are manufactured - requires an air buoyancy correction that has mass equivalent value of approximately 90 mg [4]. Given that weights can be compared on modern balances with an accuracy approaching 1 µg, and the uncertainty in the mass of kilogram 18 is around 5 µg, it is desirable to measure air density with an uncertainty of 1 part in 10^5

as this would provide an uncertainty contribution of the order of 1 μg when disseminating the kg from Pt-Ir to stainless steel standards, which is comprable with the other major uncertainty contributions. Accurate air density measurements are also required in a number of other mass related measurement applications, for example:

- When calibrating weights of International Organisation of Legal Metrology (OIML) Classes E_1 and E_2 [6].
- When measuring the mass of artefacts that are made from materials other than stainless steel [4] and uncertainties of 1 part per million (or better) are required.

In the above two examples, the accuracy of the conventional method recommended by the CIPM is adequate for the task but the cost of installing good quality temperature, pressure and humidity sensing equipment does mean that an alternative method is desirable.

2.2 The conventional method for determining air density

The density of moist air is currently determined by measuring the air temperature, pressure and humidity (and carbon dioxide concentration for best accuracy) and calculating a value for the density ρ (kg m^{-3}) using the equation recommended by the CIPM, which can expressed in the form:

$$\rho = \frac{pM_a}{ZRT}\left[1 - x_V\left(1 - \frac{M_V}{M_a}\right)\right]$$

where p is the pressure of the air in Pascals
M_a is the molar fraction of dry air in kg mol^{-1}
Z is the compressibility factor for moist air
R is the molar gas constant in J mol^{-1} K^{-1}
T is the temperature of the air in K
x_v is the molar fraction of water vapour
and M_v is the molar mass of water in kg mol^{-1}.

In practice, the calculation is more complicated since the molar fraction of water must be derived from a measurement of humidity, which in turn requires the calculation of the saturated vapour pressure of moist air [2]. Also, calculation of the compressibility Z requires a complex equation involving three quadratic functions containing four independent variables [2]. The CIPM method therefore requires accurate and demanding measurements of pressure, temperature, humidity and carbon dioxide concentration.

2.3 Shortcomings of the CIPM method

The CIPM method has a number of drawbacks which may be summarised as:

- No matter how good the ancillary equipment (temperature, pressure and humidity sensors), the absolute accuracy of the method will always be limited by the accuracy of the empirical model (the equation), which has been estimated as not exceeding 5 parts in 10^5.
- To achieve the current state-of-the-art uncertainty (~1 part in 10^4) requires the measurement of air temperature to a few mK, pressure to around 0.06 mbar and dew point (humidity) to around 0.08 °C at $k = 1$. The equipment required to meet these uncertainties is expensive and requires regular calibration to maintain its accuracy.
- The absolute accuracy of the equation has never been assessed and its uncertainty may be greater than the 5 parts in 10^5 that has been estimated.

2.4 Proposed alternative methods of air density measurement

2.4.1. Laser refractometry

The optical refractivity of air may be measured with a laser refractometer to determine variations in air density. Davidson [7] and Picard *et. al.* [8] have studied the use of laser refractometry to measure air density. Picard found that refractometry can be used to monitor changes in air density that agree to within a few parts in 10^{-6} kg m^{-3} with those values determined with the CIPM-81/91 equation. However, before a refractometer can be used to measure air density, a factor relating the air index of refraction to density must be constrained to a measurement of air density by either the use of air buoyancy artefacts or application of the CIPM-81/91 formula. Therefore, a method based on laser refractometry can only be used to determine relative measurements of air density and cannot independently provide an absolute determination.

2.4.2. Air density measurement using artefacts

The density of moist air may be measured using artefacts with a gravimetric weighing method, as described in the following chapter. Previous work at the NPL and other measurement institutes, such as the BIPM [8], have demonstrated the potential of this method. A key advantage of this approach when compared with laser refractometry is it allows an absolute determination of air density that is independent to the CIPM-81/91 equation. We propose to improve on these previous studies by performing measurements with a new set of air density artefacts that have been specifically optimised for use on the M_{one} mass comparator that is manufactured by Mettler-Toledo.

3. THE USE OF ARTEFACTS TO MEASURE AIR DENSITY

3.1 A gravimetric method to measure air density

The density of air may be determined via a gravimetric weighing method that measures the difference in the mass of air that is displaced by two artefacts of similar conventional mass and surface area but having very different volumes; this difference is proportional to the density of the air in which the artefacts are compared. Figure 1 shows a diagrammatic representation of a pair of air density artefacts with the same conventional mass and surface area that are being weighed against each other in air; the lesser apparent weight of the hollow shape artefact (pictured on the right) is a direct result of the greater mass of air that is displaced by this artefact.

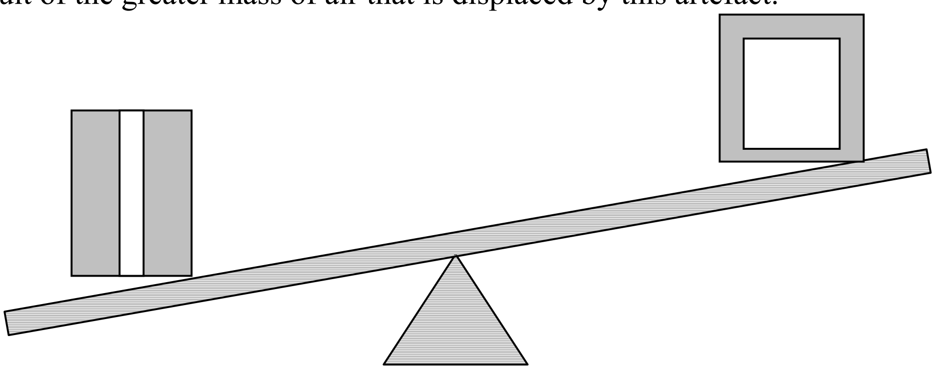

Figure 1: Hollow (right) and tube (left) shape artefacts being used for the determination of air density by gravimetric weighing

3.2 Calculation of the air density from gravimetric weighing

The calculation of the density of air requires values for the following parameters:

ΔM_T - The mass (g) of the large volume artefact less the mass of the small volume artefact; this value is determined by the comparison weighing of the two artefacts in a vacuum environment. If the two artefacts are manufactured from different materials and/or have different surface areas then a sorption correction must be applied to account for moisture and other contaminants that absorb on the artefact surfaces upon their transfer from vacuum to ambient air.

ΔW_A - The weight (g) of the large volume artefact less the weight of the small volume artefact in the air whose density is to be determined. This weight difference is uncorrected for the buoyancy of the air.

ΔV – The volume (cm^3) of the large volume artefact less the volume of the small volume artefact (note: the volumes are corrected using values for the thermal coefficient of expansion for each artefact).

Values for these parameters are used in the following equation to calculate the density of the ambient air ρ_a (g cm^{-3}):

$$\rho_a = \left(\frac{\Delta M_T - \Delta W_A}{\Delta V} \right)$$

3.3 Historical development of air density artefacts at NPL

The first studies (in 1994) using air density artefacts at the NPL involved the manufacture of a spherical and hemispherical artefact with a volume difference of around 760 cm^3 (see Figure 2). At this time, there was no facility at the NPL for weighing artefacts in vacuum and so they were designed to be assembled from matched components to ensure their masses and internal and external surface areas were closely matched (see Figure 3). The component masses were determined prior to their assembly and ΔM_T subsequently calculated.

Figure 2: Mk I air density artefacts manufactured at NPL in 1994

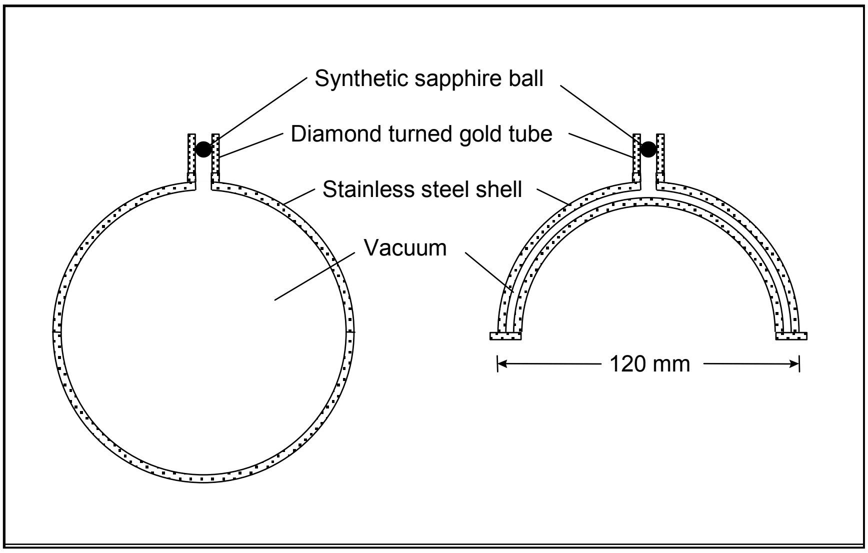

Figure 3: Components of the Mk I artefacts

During assembly, the air within the artefacts was evacuated and the cavities sealed with balls made from sapphire. Once assembled, a value for ΔM_A could be determined by the comparison weighing of the artefacts in air to an uncertainty of approximately 10 µg which, coupled with their relatively large volume difference, meant the potential uncertainty in the air density measurement would be around 1 part in 10^5. Unfortunately, in their use, it was discovered that the mass stability of the artefacts was poorer than anticipated and was later attributed to the relatively poor surface finish that could be achieved on the spherical surfaces. Mass changes of about 100 µg were seen over a period of about 12 months and the air density calculated with these artefacts was found to disagree with the CIPM method by 5 parts in 10^4[7].

3.4 Next generation NPL air density artefacts

Custom designed artefacts, manufactured from non-magnetic stainless steel, were purchased from Precisa Balances Ltd. Two different sets of artefacts were built, each comprising two bobbin shaped artefacts and two hollow cylindrical artefacts. At a later date, two tube shaped artefacts were also manufactured for each set:

- Set NPLW81 was comprised of six artefacts with diameters ranging from 49 mm to 60 mm, and a height of 84 mm, for use with commercial automatic balances. These artefacts are referred to as 81bobbin & 81Dbobbin (bobbin shaped), 81tube & 81Dtube (tube shaped) and 81hollow & 81Dhollow (hollow cylinder);
- Set NPLW88 was comprised of six artefacts with diameters ranging from 68 mm to 90 mm, and a height of 100 mm, for use on a Mettler Toledo M_{one} balance. These artefacts are referred to as 88bobbin & 88Dbobbin (bobbin shaped), 88tube & 88Dtube (tube shaped) and 88hollow & 88Dhollow (hollow cylinder).

Artefacts from each set are shown in Figure 4. The advantage of using the physically larger artefacts that comprise set NPLW 88 is the large volume difference of ~510 cm^3 that has been obtained between the artefacts, which compares with ~104 cm^3 for the artefacts of set NPLW 81 that have been designed for use with commercially available balances. The larger volume difference means the air density has the potential to be measured with a lower uncertainty of around 1 in 10^5, which compares with 5 in 10^5 for the smaller artefacts. A disadvantage of using larger artefacts is they can only be used on balances that have sufficient space to accommodate these artefacts on their weighing pans (e.g. such as the Mettler M_{one} balance that is used for the work reported here).

Figure 4: Large (back) and small (front) air density artefacts. From left to right: hollow shape, tube shape and bobbin shape

4. CONVECTION EFFECTS ON AIR DENSITY ARTEFACTS

4.1 Free convection effects on standard weights

Gläser [9] has shown that convection effects can occur at a weights surface due to heating or cooling of the air, particularly when the weight has a different temperature from that of its ambient surroundings. In the case of a weight being measured on a balance equipped with a turntable for the automatic exchange of weights, free convective air flow would be expected to follow a path across the turntable and up along the vertical surface of the weight before separating at some point on the weight's top surface (see Figure 5). Davidson *et. al.* [10] have measured the temperature at different elevations within the enclosed environment of a Mettler-Toledo AT10005 mass comparator with an automatic weight exchanger; they found temperature gradients that would result in convective airflow and therefore modify the apparent weight of the artefacts.

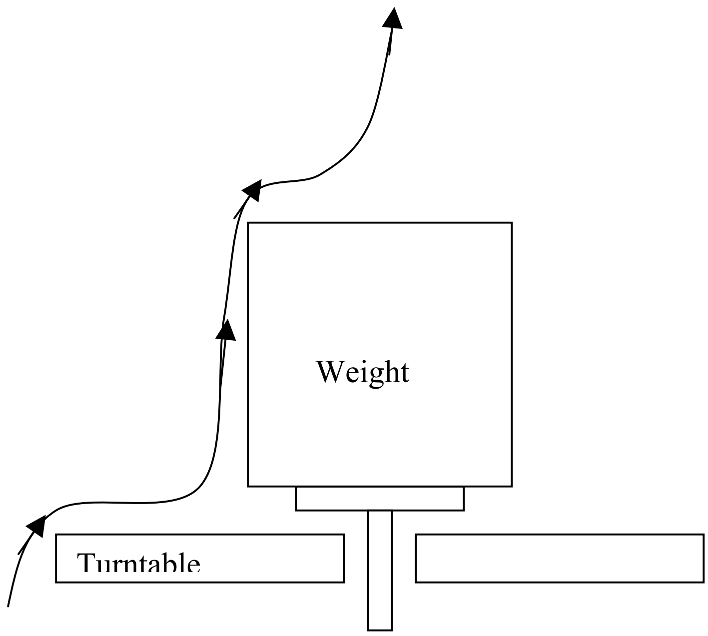

Figure 5: Convective air flow path over a weight located on a balance with a turntable for the automatic exchange of weights

4.2 Measurements in ambient air of set NPLW 81

As described in §3.1, the measurement of the density of air requires two artefacts with a significantly large volume difference. Two geometries for the small volume artefacts were designed and manufactured; a tube and a bobbin shape (see Figure 4). The effectiveness of these artefacts were investigated by performing two experimental weighings of all the artefacts that comprise set NPLW 81 using the Mettler-Toledo M_{one} balance. Weighing 1 comprised a series of 20 measurements per comparison over a 48 hour period, and weighing 2 comprised 64 measurements per comparison over a 76 hour period. The standard deviations of the comparisons are given in Table 1.

Weighing 1	
Comparison	**σ_{n-1} (µg)**
81hollow – 81tube	4.5
81Dhollow – 81tube	3.4
81hollow – 81Dtube	4.4
81Dhollow – 81Dtube	3.5
81hollow – 81bobbin	10.5
81Dhollow – 81bobbin	7.1
81hollow – 81Dbobbin	9.7
81Dhollow – 81Dbobbin	7.8
Weighing 2	
Comparison	**σ_{n-1} (µg)**
81hollow – 81tube	4.2
81Dhollow – 81tube	4.2
81hollow – 81Dtube	5.0
81Dhollow – 81Dtube	4.9
81hollow – 81bobbin	8.3
81Dhollow – 81bobbin	7.7
81hollow – 81Dbobbin	8.7
81Dhollow – 81Dbobbin	8.6

Table 1: Standard deviation of ambient air measurements on set NPLW 81 - small air density artefacts

The results show that higher standard deviations (ranging from 7.1 to 10.5 µg) were obtained for the comparison weighings of the bobbin and hollow cylindrical artefacts than those of the tube and hollow cylindrical artefacts (3.4 to 5.0 µg). This would indicate that the tube shaped artefacts are more suitable than the bobbin shaped artefacts for use as the small volume counterparts to the hollow cylindrical artefacts. As both of the small volume artefacts have similar surface areas and volumes it seems likely that their shapes are responsible for the difference in their performance.

4.3 Computational Fluid Dynamic (CFD) analysis on air density artefacts

4.3.1. CFD boundary conditions and modelling assumptions

The observed difference in the weighing standard deviations reported in Table 1 may be due to variations in airflow across the surfaces of the tube and bobbin artefact caused by their differences in geometry. From the theory describing convective air flow (§4.1), it would seem likely that during the weighings convective air flow patterns would have occurred over the surfaces of the hollow, bobbin and tube shaped air density artefacts. It is postulated that this convective effect was responsible for the difference in the experimental results. To ascertain the likelihood of this postulation, computational models of the hollow, bobbin and tube artefacts within an ambient air environment were constructed using ANSYS version 5.4 Computational Fluid Dynamics (CFD) software.

The average vertical temperature gradient was measured across the weighing region of the Mettler-Toledo M_{one} balance and was found to be +32.5 mK (reported in §5.2.1). Applying this value for the temperature gradient, and a characteristic length of 0.144 m - a combination of the height 0.084 m and diameter 0.060 m of a small air density artefact - to the formula used to calculate the mean velocity of airflow at a vertical surface (derived by Gläser [9]) gives a mean velocity of approximately 0.004 ms^{-1}. A 2-D CFD model (shown in Figure 6) was then constructed by assigning the following boundary conditions:

1. uniform vertical air flow V_y of 0.004 ms^{-1} at the model inlet;
2. no-slip wall conditions were specified by taking the airflow to be zero in the x and y directions;
3. zero pressure degree of freedom at the flow outlet.

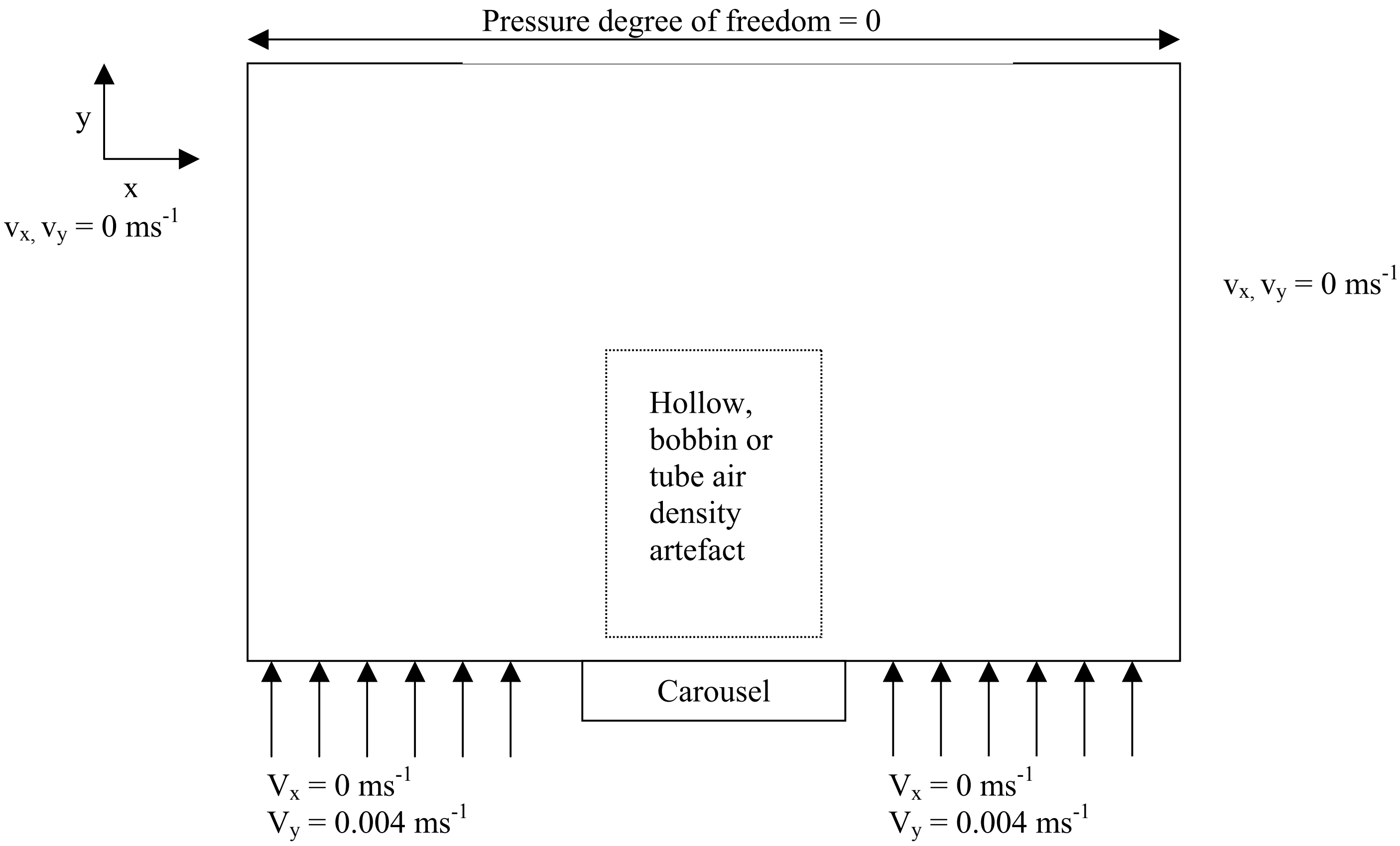

Figure 6: Boundary conditions assigned to the CFD models of the ambient air flow around hollow, tube and bobbin shape air density artefacts

A region within the model representing a carousel for the automatic exchange of weights was constructed and each design of air density artefact was incorporated into the model at a distance of 0.005 m above the carousel. In reality, a balance pan would support the artefacts at this distance above the carousel but has been omitted from the model as the pan is unlikely to have a significant effect on the airflow around the artefacts. The carousel on an actual balance would also have cut-outs (shown in Figure 7) to enable the weighing pan to pick up artefacts and it is likely that some airflow would occur through them. A further complication is that within an actual balance it is unlikely that the airflow would have a uniform velocity at one particular cross-section of the balance as assumed in the computational model. However, the aim of this CFD study is not to produce a perfect model of the balance and its environment but to instead highlight differences in airflow across the surfaces of the differently shaped artefacts, and so it was considered acceptable to leave out these details to simplify the model.

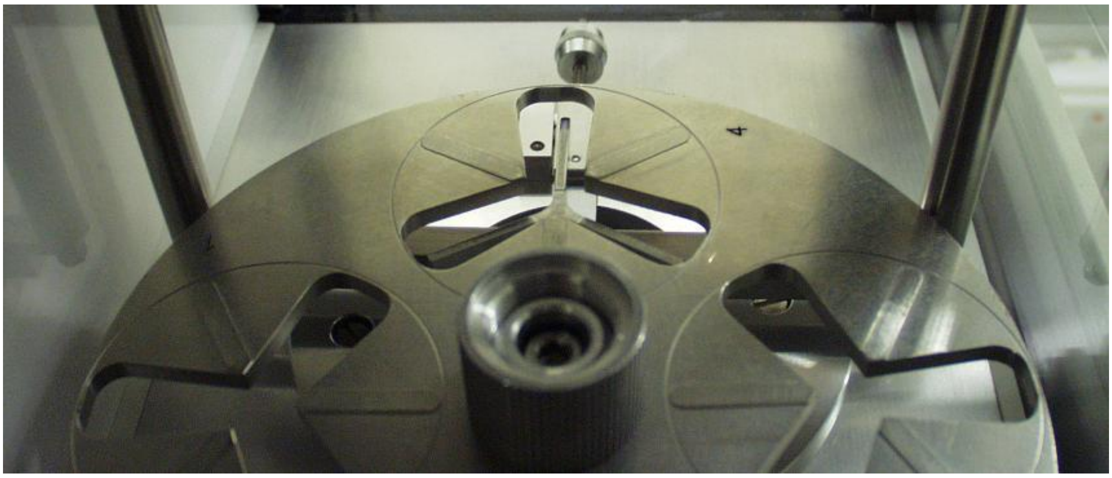

Figure 7: View of the carousel and weighing pan of a Mettler HK1000 mass comparator

4.3.2. CFD calculated air velocity profile around air density artefacts

Velocity profile plots were created from the results of the CFD analysis for the hollow (Figure 8), tube (Figure 9) and bobbin (Figure 10) shape artefacts.

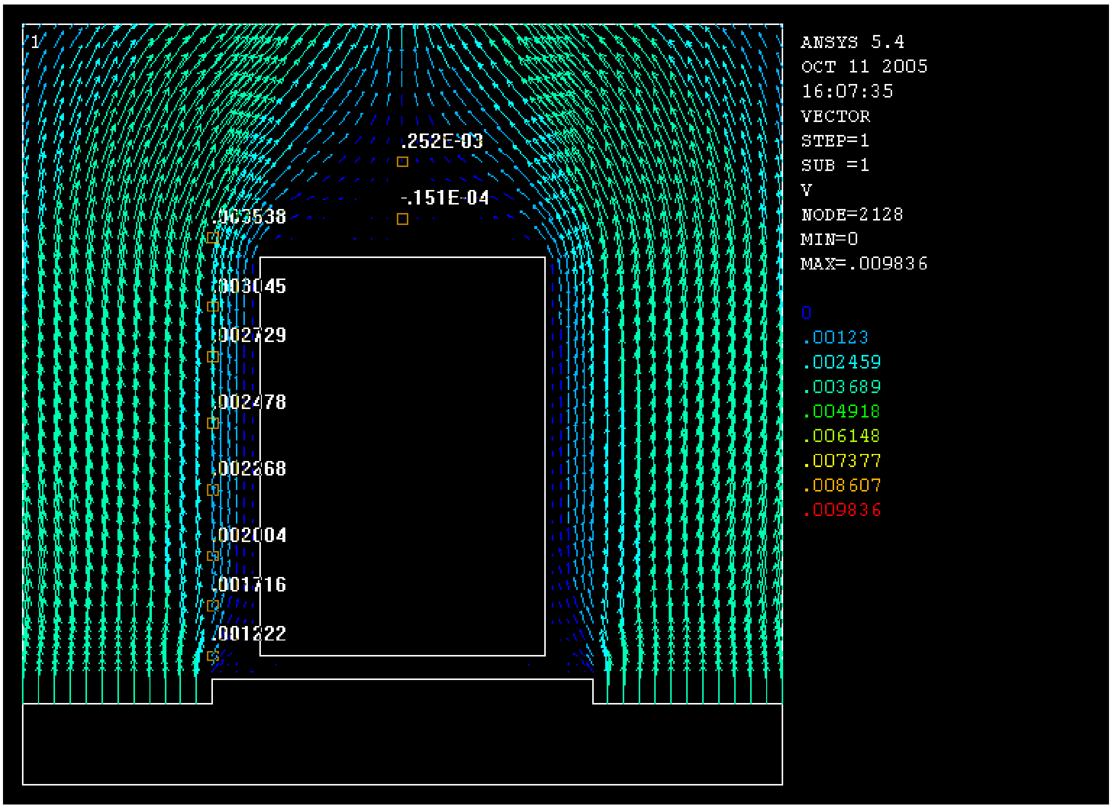

Figure 8: Velocity profile plot of the airflow around the hollow shape air density artefact

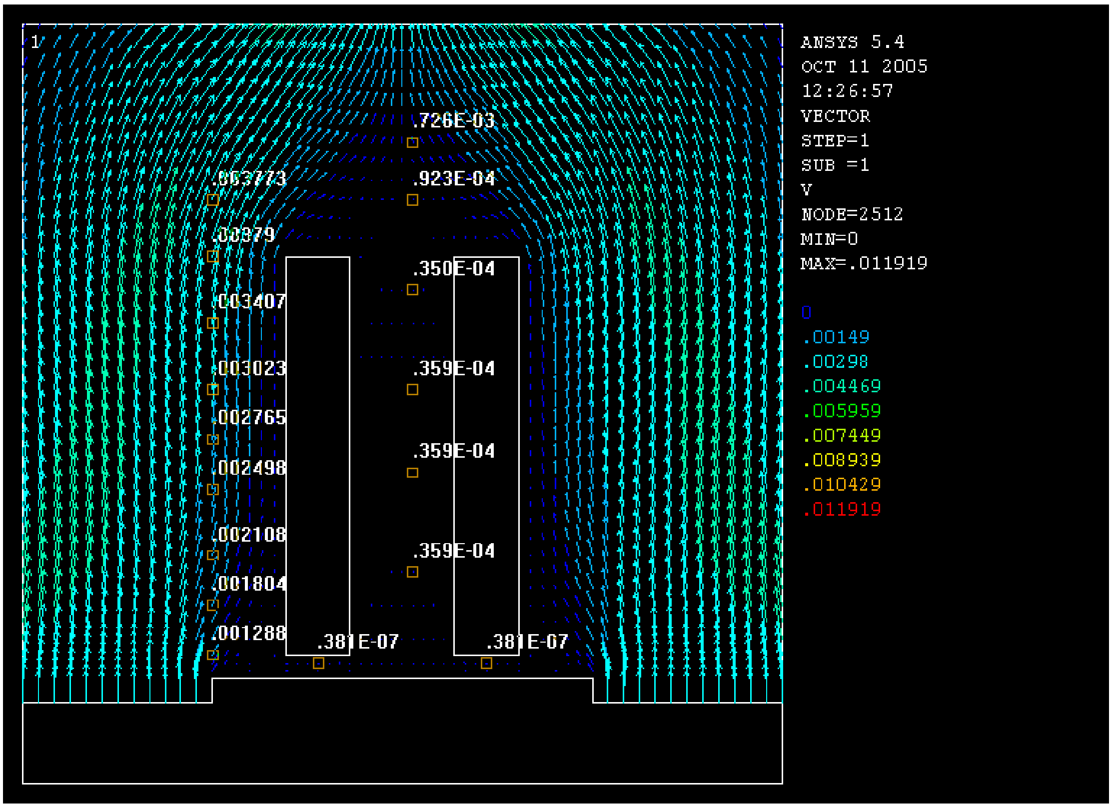

Figure 9: Velocity profile plot of the airflow around the tube shape air density artefact

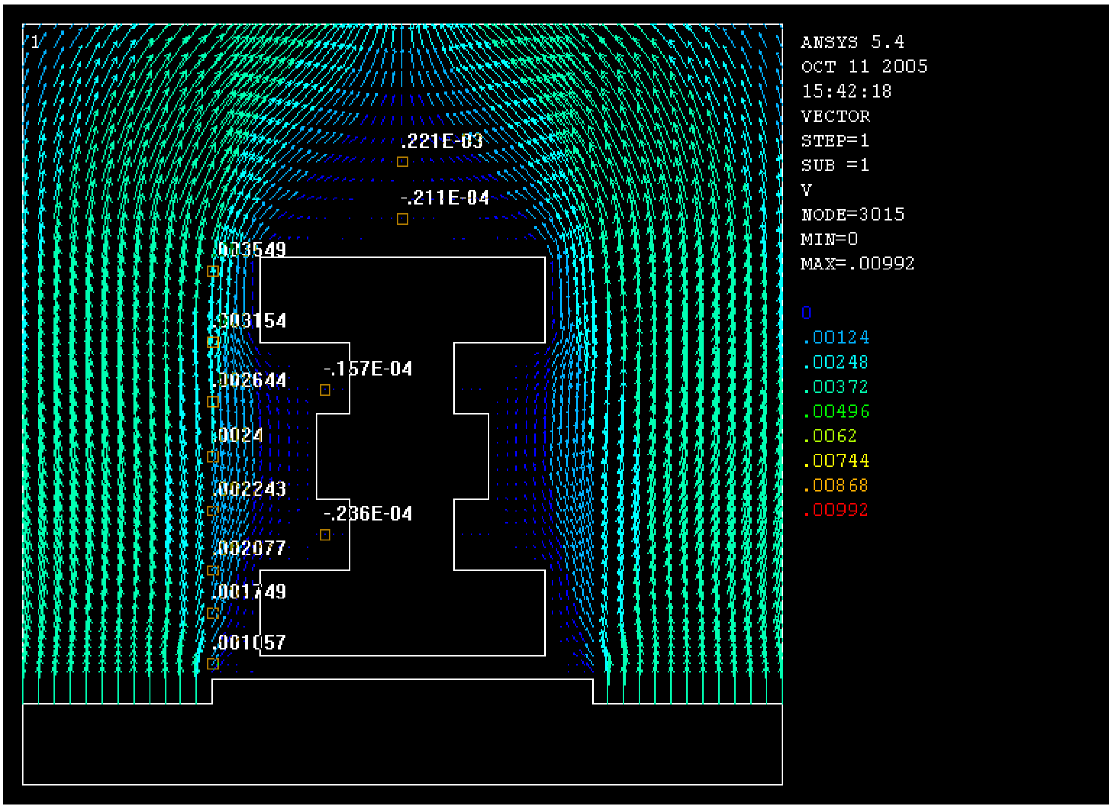

Figure 10: Velocity profile plot of the airflow around the bobbin shape air density artefact

The CFD velocity profile shows that laminar flow occurs over the vertical surfaces of the hollow (Figure 8) and tube (Figure 9) shape air density artefacts, with small eddies forming over the top surface of the hollow shape as a likely result of the flow separating from it's surface. A small flow of approximately 0.000 35 ms^{-1} was evident through the centre of the tube shape artefact, which could induce a small viscous drag and hence impart a small reaction lift force upon the artefact. In practice, however, as this flow is less than one tenth of the flow around the outer surface it is unlikely to have a significant effect on the overall forces acting upon the artefact. Thus, as long as there is little possibility of flow through the centre of the tube shape artefact, then changes in ambient environmental conditions are likely to affect the tube in the same manner as they would affect the hollow shape artefact.

Examining the velocity profile of the airflow around the bobbin shape artefact (Figure 10) it can be seen that the top surface of the bobbin behaves in a similar manner to that of the hollow shape as small eddies occur due to the flow separating from its surface. However, the flow around the side of the bobbin artefact differs significantly from that of the hollow and tube shape artefacts, in that it bows around the cut-out sections resulting in the formation of eddies as indicated by the negative sign on the velocity profile plot (Figure 10). It is likely that these eddies produce a pressure effect that results in reaction forces upon the bobbin and therefore causes a change in the apparent mass of the bobbin on the weighing pan. The CFD modelling therefore provides an explanation for the higher standard deviations reported in Table 1. *As a result of the CFD modelling and the experimental measurements, a decision was made to use the tube shape artefacts as counterparts to the hollow shapes in preference to the bobbin shape artefacts.* Also, two new large tube shaped artefacts were designed and manufactured to replace the large bobbin shaped artefacts in set NPLW 88.

5. EXPERIMENTAL MEASUREMENTS

5.1 Density, volume and coefficient of thermal expansion of the artefacts

Table 2 reports values for the density, volume and coefficient of thermal expansion for the artefacts of sets NPLW 81 and 88. The volumes and coefficients of thermal expansion were measured using the NPL 1 kg hydrostatic weighing apparatus.

Identification	Density @ 20 °C	Density uncertainty 2 σ	Volume @20 °C	Volume uncertainty 2 σ	Coefficient of thermal expansion
	g cm^{-3}	g cm^{-3}	cm^3	cm^3	10^{-6} °C^{-1}
81bobbin	8.011 18	0.000 15	124.825 5	0.002 4	45.5
81Dbobbin	8.011 10	0.000 15	124.826 8	0.002 4	45.5
81hollow	4.363 87	0.000 07	229.181 3	0.003 7	45.5
81Dhollow	4.214 50	0.000 06	237.307 0	0.003 4	45.5
81tube	8.007 41	0.000 18	124.884 4	0.002 8	42.8
81Dtube	8.007 41	0.000 17	124.884 4	0.002 7	42.8
88bobbin	8.012 26	0.000 17	124.808 7	0.002 7	43.0
88Dbobbin	8.012 43	0.000 15	124.806 1	0.002 4	43.0
88hollow	1.573 50	0.000 02	635.524 2	0.008 1	47.8
88Dhollow	1.576 98	0.000 02	634.122 1	0.008 1	47.8
88tube	8.011 09	0.000 16	124.826 9	0.002 5	44.2
88Dtube	8.011 06	0.000 15	124.827 5	0.002 4	44.2

Table 2: Density, volume and coefficient of thermal expansion of the NPL air density artefacts

5.2 Air temperature, pressure, humidity and carbon dioxide concentration

Measurements of the air temperature, pressure, humidity (calculated from the temperature and dew point of the ambient air) and carbon dioxide concentration are required to determine the air density using the CIPM method (§2.2). The temperature measurements are also used when determining the correction to the volumes of the air density artefacts to account for their thermal expansion.

5.2.1. Temperature measurement

The air temperature within the balance enclosure was measured with two calibrated 100 Ω platinum resistance thermometers (PRTs) and a calibrated commercial bridge that has a resolution of 0.2 mK. One PRT was placed level with the weighing pan, whilst the second was mounted 12.5 cm higher. The average temperature difference between the two PRTs was recorded over a 24-hour period and was found to be 32.5 mK (± 2.1 mK).

5.2.2. Pressure measurement

Measurement of air pressure was made using a calibrated digital barometer with a resolution of 0.01 mbar. No correction for the elevation was needed as the barometer was mounted level with the weighing pan of the M_{one} balance.

5.2.3. Humidity measurement

The humidity inside the balance enclosure was measured using a calibrated dew point hygrometer with a resolution of 0.01 ° C.

5.2.4. Carbon dioxide concentration measurement

Measurement of the concentration of CO_2 in the air within the balance enclosure was made with a checked carbon dioxide meter that has a resolution of 1 ppm. The zero indication of the meter was checked prior to its use by filling the chamber with oxygen-free dry nitrogen, whilst the span was checked by filling the chamber with Nitrogen gas containing a certified CO_2 concentration of 411 ppm.

5.3 Mass measurements in vacuum

The measured mass differences in vacuum ΔM_T (see §3.2) are reported in Table 3, and were determined using a Mettler-Toledo M_{one} balance at pressures below 0.1 Pa. The artefacts were left to stabilise within the vacuum environment for a period of 24 hours prior to making the measurements.

Comparison in Vacuum	Mass difference (mg)	Standard Deviation (µg)
88hollow – 88tube	-0.323 5	1.5
88hollow – 88Dtube	0.238 7	1.4
88Dhollow – 88tube	-1.666 6	1.4
88Dhollow – 88Dtube	-1.577 7	1.7

Table 3: Mass differences (in vacuum) between large and small volume air density artefacts that comprise set NPLW 88. These values were determined on 7 April 2005

5.3.1. Mass stability of set NPLW 88

Knowledge of the stability of ΔM_T is important as variations in this value directly effect the calculated air density. The variations in ΔM_T for set NPLW 88 were measured over a period of 261 days, and are reported in Figure 11 and Figure 12. The artefacts were stored in standard atmospheric pressure between the measurements.

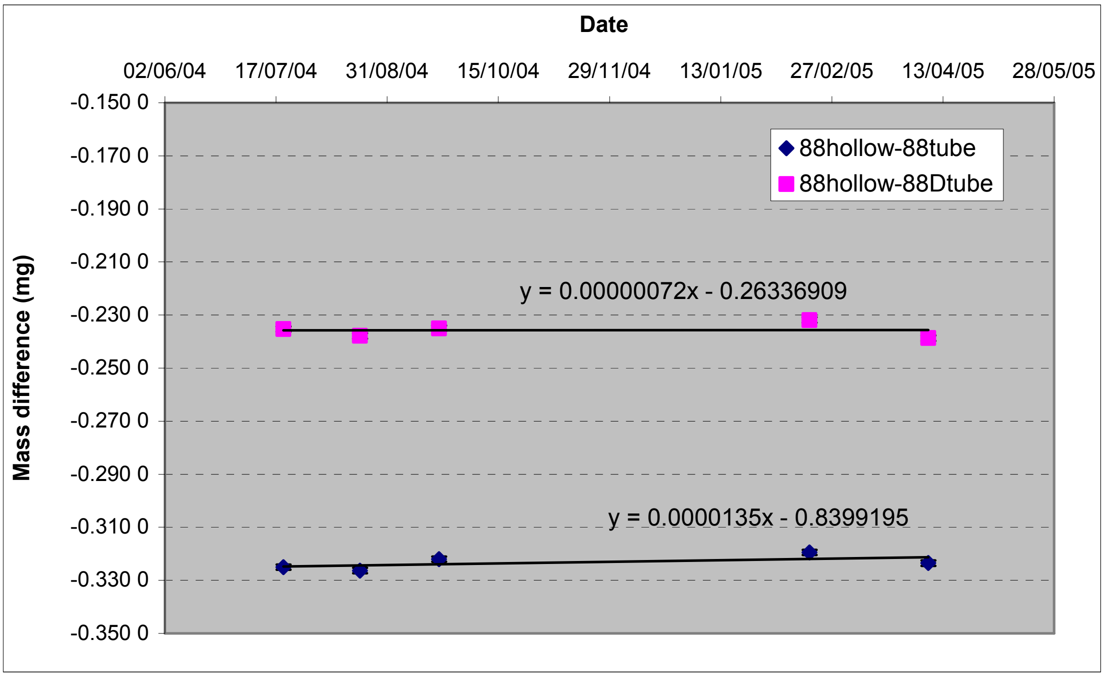

Figure 11: Mass stability of 88hollow relative to 88tube and 88Dtube as a function of time. Uncertainty bars represent the experimental standard deviation

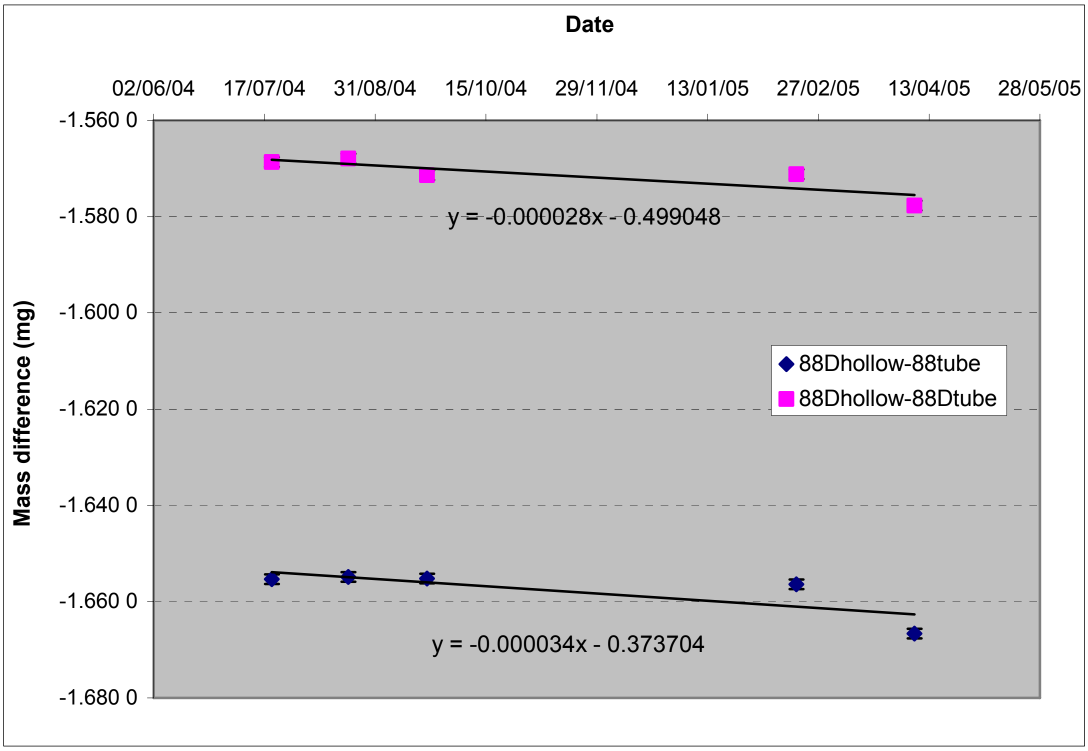

Figure 12: Mass stability of 88Dhollow relative to 88tube and 88Dtube as a function of time. Uncertainty bars represent the experimental standard deviation

Figure 12 shows good stability in the mass difference between both sets of air density artefact (drift in mass difference is about 10 μg per year). This is important, as the mass stability of the artefacts is a significant component in the uncertainty in their measurement of air density (§ 5.5.2). A linear fit has been applied to the data to predict the change in ΔM_T with time and the fitted coefficients are displayed on the graphs. The uncertainties in the best-fit line have been evaluated and are shown in Table 4 and include contributions from the standard error of the fitted data and the uncertainty of the weighing scheme.

	88hollow – 88tube	**88hollow – 88Dtube**	**88Dhollow – 88tube**	**88Dhollow – 88Dtube**
Stability uncertainty (mg/year)	0.0038	0.0046	0.0053	0.0036

Table 4: Uncertainty in the fitted prediction of the mass difference variation

5.4 Air density measurements using set NPLW88

5.4.1. Artefact versus CIPM-81/91 method

Six separate measurements of the density of moist air were made using the artefacts from set NPLW 88 and the CIPM equation. An ABA weighing scheme was used for the artefact measurements, and a value of air density calculated from the resulting mass difference. The corresponding air density calculated using the CIPM method was taken at the mid point of each ABA weighing. Table 5 reports the average values obtained with each method. The air density values determined with the artefacts were found to be consistently higher that those calculated from the CIPM equation, with the average difference being 16×10^{-5} kg m^{-3}. *This is a significant discrepancy as the uncertainty in the CIPM-81/91 method has been estimated as* 11×10^{-5} *kg m*$^{-3}$ [k = 1] (taken from the uncertainty budget given in §5.5.1).

Date	**Average air density {Artefacts}** (kg m^{-3})	**Average air density {Equation}** (kg m^{-3})	**Difference {Artefact - Equation}** (kg m^{-3})
25 Aug 04	1.187 63	1.187 52	1.1×10^{-4}
3 Sept 04	1.203 96	1.203 79	1.7×10^{-4}
7 Sept 04	1.219 13	1.218 96	1.7×10^{-4}
15 Nov 04	1.218 40	1.218 19	2.1×10^{-4}
6 Dec 04	1.216 43	1.216 27	1.6×10^{-4}
10 Dec 04	1.214 16	1.214 00	1.6×10^{-4}
Average difference			**1.6×10^{-4}**

Table 5: Average values of the air density determined with the artefacts and the CIPM method

5.4.2. Argon and CO_2 anomalies

Park *et. al.* [5] have recently reported a new value for the argon content of standard air and, in response to this new data, Picard *et. al.* [11] have investigated its impact on the CIPM-81/91 equation and concluded by suggesting that this method underestimates the air density by 7.7×10^{-5} kg m^{-3}. A modification to the CIPM-81/91 equation to account for the new argon content of air would therefore reduce the discrepancy between the air density artefacts and the CIPM-81/91 method to 8.3×10^{-5} kg m^{-3}.

Measurements of the CO_2 concentration within the sealed chamber of the M_{one} balance showed concentrations as high as 600 ppm. Previously, it has been assumed that the CO_2 concentration would remain relatively constant at around 400 ppm and therefore a value of 400 ppm could be assumed when determining the air density with the CIPM-81/91 method. An error of +200 ppm in the value of the CO_2 content used in the CIPM-81/91 equation would underestimate the air density by 10.2×10^{-5} kg m^{-3}. Thus, the difference between the air density artefacts and the CIPM-81/91 method is reduced to -1.9×10^{-5} kg m^{-3} when corrections have been applied for the argon and CO_2 concentrations, which is small compared with the uncertainty in the CIPM-81/91 determination (11×10^{-5} kg m^{-3}).

5.4.3. Artefact versus corrected CIPM-81/91 method

Discrepancies in the determination of air density by the artefact and the CIPM-81/91 methods have been explained by the incorrect assumption of a value for the CO_2 concentration in air, and a revised value for the amount of argon present in ambient air. These two sources of error were addressed by: 1) equipping the balance chamber with a calibrated CO_2 meter (see §5.2.4) and modifying the software that calculates air density from the CIPM-81/91 equation to read values of CO_2 from the meter; and 2) changing the argon content used by the CIPM-81/91 equation to the new argon content value of 9.332 mmol mol^{-1}, as determined by Park *et. al.* [5].

Seven new measurements of the air density were made, and the difference between the artefacts and the modified CIPM-81/91 method evaluated and summarised in Table 6. The data in Figure 3 shows the variation in air density during one of these measurements; the error bars represent the uncertainty obtained with the modified CIPM-81/91 method. The agreement between the artefacts and the modified CIPM-81/91 method is well within the uncertainty of the modified CIPM-81/91 method.

Date	Air density difference {Artefacts – modified CIPM-81/91 method} (kg m^{-3})
19 Apr 05	3.0×10^{-5}
20 Apr 05	5.0×10^{-5}
25 Apr 05	0.0×10^{-5}
26 Apr 05	2.0×10^{-5}
27 Apr 05	2.0×10^{-5}
28 Apr 05	-1.0×10^{-5}
29 Apr 05	1.0×10^{-5}
Average difference	$\mathbf{2.0 \times 10^{-5}}$
Standard deviation	$\mathbf{2.0 \times 10^{-5}}$

Table 6: Difference in the values of the air density determined with the artefacts and the modified CIPM-81/91method

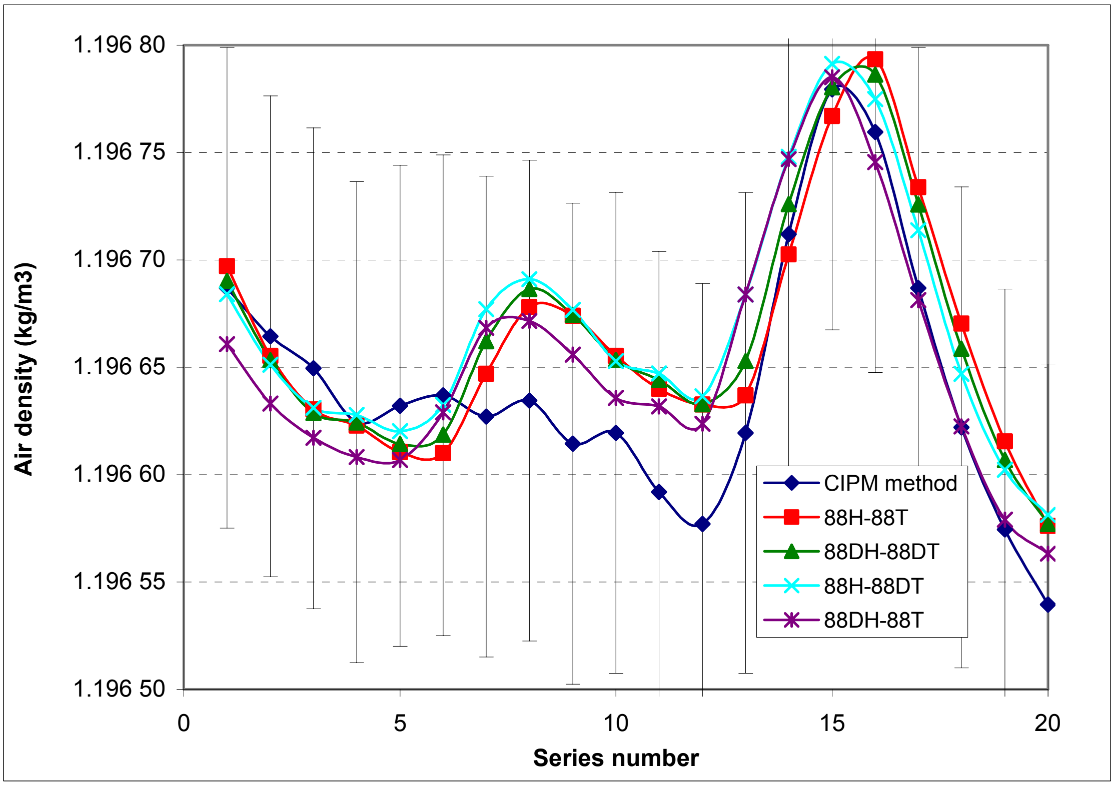

Figure 13: Comparison of air density measured using the modified CIPM-81/91 method and the air density artefacts

The average difference between the artefacts and the modified CIPM-81/91 method values was found to be 2.0×10^{-5} kg m^{-3}, with a standard deviation of 2.0×10^{-5} kg m^{-3}. *These two values are well within the 11.0×10^{-5} kg m^{-3} uncertainty [k = 1] (see §5.5.1) attributable to the modified CIPM-81/91 method and, therefore, good* *agreement has been achieved between the two techniques, which has validated the artefacts' ability to measure air density.* It is worth noting that it takes several minutes to measure a value of air density using the artefacts, and the difference between the methods was found to increase when they are used to measure the air density within an unsealed environment. *It is therefore only advantageous to use the air density artefacts within a hermetically sealed environment.*

5.5 Uncertainties

Uncertainty budgets for the two methods are summarised below:

5.5.1. Uncertainty in the air density measurement using the CIPM-81/91 method

Parameter	**Standard Uncertainty, u_i**		**Relative influence, $u_i(\rho)/\rho$**	
	Type A	**Type B**	**Type A**	**Type B**
Pressure (Pa)				
Acquisition	1.00	-	0.12×10^{-4}	-
Calibration	-	6.00	-	0.71×10^{-4}
Height correction	-	-	-	-
Dew point (K)				
Acquisition	0.010	-	0.03×10^{-4}	-
Calibration	-	0.080	-	0.28×10^{-4}
CO_2 (ppm)				
Acquisition	1.0	-	0.01×10^{-4}	-
Calibration	-	50.0	-	0.25×10^{-4}
Temperature (mK)				
PRT acquisition	0.20	-	0.01×10^{-4}	-
PRT calibration	-	2.50	-	0.10×10^{-4}
Std resistor - acquisition	0.20	-	0.01×10^{-4}	-
Std resistor - calibration	-	0.00	-	0.00×10^{-4}
Equation (kg m^{-3})	0.30×10^{-4}	0.70×10^{-4}	0.25×10^{-4}	0.60×10^{-4}
Subtotal			0.28×10^{-4}	1.01×10^{-4}
Relative combined uncertainty, u_c (kg m^{-3})				**1.05×10^{-4}**

Table 7: Uncertainty budget for the air density measurement using the CIPM-81/91 method. The uncertainty in the equation is taken as the value reported by Picard and Fang [5]. All uncertainties are reported at the 1 σ level

Table 7 shows the relative combined uncertainty is 1.05×10^{-4} kg m^{-3}, and the main contributions arise from the measurement of pressure and the equation.

5.5.2. Uncertainty in the air density measurement using the artefacts

Parameter	Standard uncertainty u_i	Relative influence $u_i(\rho)/\rho$
Vacuum mass (µg)		
Weighing scheme Sorption correction Stability of ΔM_T	1.40 0.00 3.10	0.2×10^{-5} 0.0×10^{-5} 0.5×10^{-5}
Air mass (µg)		
Weighing scheme	1.40	0.2×10^{-5}
Volume (cm^3)	0.004 21	0.8×10^{-5}
Relative combined uncertainty, u_c (kg m^{-3})		$\mathbf{1.1 \times 10^{-5}}$

Table 8: Uncertainty budget of air density evaluation using the artefact method. All uncertainties are reported at the 1 σ level

Table 8 shows the main contributions to the uncertainty arise from the stability of ΔM_T and the volume determination of the artefacts. The stability of ΔM_T has been estimated from a one-month period where the artefacts were exposed to vacuum on 5 occasions. This uncertainty component can be reduced if the artefacts are calibrated on a more frequent basis, and even more so if the artefacts are calibrated immediately prior to their use to measure air density.

5.5.3. Reduced uncertainty in the dissemination of the mass scale at 1 kg

Table 9 shows the combined uncertainty in the dissemination of the mass scale from a Pt-Ir mass to a stainless steel mass at 1 kg. The uncertainty in the calibration of the stainless steel 1 kg standard has been halved when the air density is measured with the artefacts.

Uncertainty components	**CIPM-81/91 method uncertainty** (± mg)	**Artefact method uncertainty** (± mg)
Air density	0.008 5	0.000 9
Pt-Ir standard	0.005 2	0.005 2
Weighing scheme (including balance uncertainty)	0.001 4	0.001 4
Make weights	0.000 2	0.000 2
Relative combined uncertainty	**0.010 0**	**0.005 5**

Table 9: Uncertainty budget example for the calibration of a stainless steel mass from a Pt-Ir standard mass. All uncertainties are reported at the 1 σ level

6. CONCLUSIONS

NPL has designed and evaluated two sets of air density artefacts. Each set is comprised of two hollow cylindrical shape artefacts, two bobbin shape artefacts and two tube shape artefacts. Computational fluid dynamic (CFD) modelling has been used to evaluate the airflow around the different shape air density artefacts. The output from the CFD modelling, and the results from experimental weighings, have demonstrated that the tube shape is better suited to air density measurement than the bobbin shape.

Measurements of the air density made with the artefacts and the CIPM-81/91 method (modified for a new value of argon concentration and to measure the CO_2 concentration in the balance enclosure) have shown an excellent agreement of 2 parts in 10^5, which is less than one fifth of the overall estimated uncertainty in using the modified CIPM-81/91 method. Furthermore, the uncertainty in the measurement of air density using the artefacts has been estimated as 1.1 parts in 10^5, which is nearly a ten-fold reduction compared with the CIPM-81/91 method. This reduction will enable the overall uncertainty in calibrating stainless steel 1 kg weights from primary platinum-iridium standards to be reduced by 50%. However, as it takes several minutes to weigh each artefact and determine a value for air density, the advantages of using artefacts over the modified CIPM-81/91 method are only attainable when the atmospheric conditions are stable e.g. when the balance is located within a hermetically sealed chamber.

7. ACKNOWLEDGEMENTS

The authors acknowledge the financial support of the National Measurement System Directorate of the UK Department of Trade and Industry.

8. REFERENCES

[1] Giacomo P 1982 Metrologia 18 33-40

[2] Davis R S 1992 Metrologia 29 67-70

[3] Severn I 2004 NPL Report MATC(A)166

[4] Davidson S et al 2004 NPL Good Practice Guide No. 71

[5] Park et al 2004 Metrologia 41 387-395

[6] OIML R111-1 2004 OIML

[7] Davidson S 2000 XVI IMEKO World Congress Proceedings Volume III 29-34

[8] Picard A and Fang H 2002 Metrologia 39 31-40

[9] Gläser M 1999 Metrologia 36 183-197

[10] Davidson S, Peattie G, Buckley M and Palmer D 2001 NPL Report CMAM 74

[11] Picard A, Fang H and Gläser M 2004 Metrologia 41 396-400